Chapter 1

Vesicle Reconstitution & Characterization of the Synthetic Mechanosensitive Channel of Large Conductance

1.1 Introduction

Mechanosensation is used in all three kingdoms of life for various functions. In bacteria, mechanosensation is necessary to regulate osmotic pressure and prevent lysis of the cell wall. Three distinct ion channels have been classified by their conductance in bacteria. The mechanosensitive channel of large conductance (MscL) has a conductance > 1 nS, the mechanosensitive channels of small conductance (MscS and MscK) have conductances between 0.3–0.5 nS, and the mechanosensitive channel of mini conductance (MscM) has a conductance between 0.1–0.15 nS (1–4). *E. coli* MscL was first cloned in 1994 and experiments explicitly showed that mechanosensation through the lipid bilayer could be performed by a single ion channel (5).

Rees and co-workers solved the crystal structure of MscL from *Mycobacterium tuberculosis* (Tb-MscL). The crystal structure revealed a channel formed by a homopentamer, where each subunit contained two transmembrane (TM) α helices and a third cytoplasmic α helix (Figure 1.1). The structure lacks the first 9 residues in the N-terminus and 33 residues in the C-terminus (6). Tb-MscL has sequence homology of 37% when compared to the *E. coli* MscL (Ec-MscL), with highest homology in the TM regions (7). MscL is thought to serve as a sensor for changes in osmolarity because the channel is gated by tension, through the lipid bilayer, that is near the lytic limit of most bacterial cells (1,8). Upon tension gating, MscL generates a large conductance of ≈ 3 nS, with multiple sub-conductance states (9,10). Synthetic MscL samples were prepared containing a N-terminal biotin moiety (B-Ec-MscL & B-Tb-MscL) (11) and this research was performed to reconstitute the channel into vesicles for characterization within the

lipid bilayer, analysis of the oligomeric state, and channel function through electrophysiology.

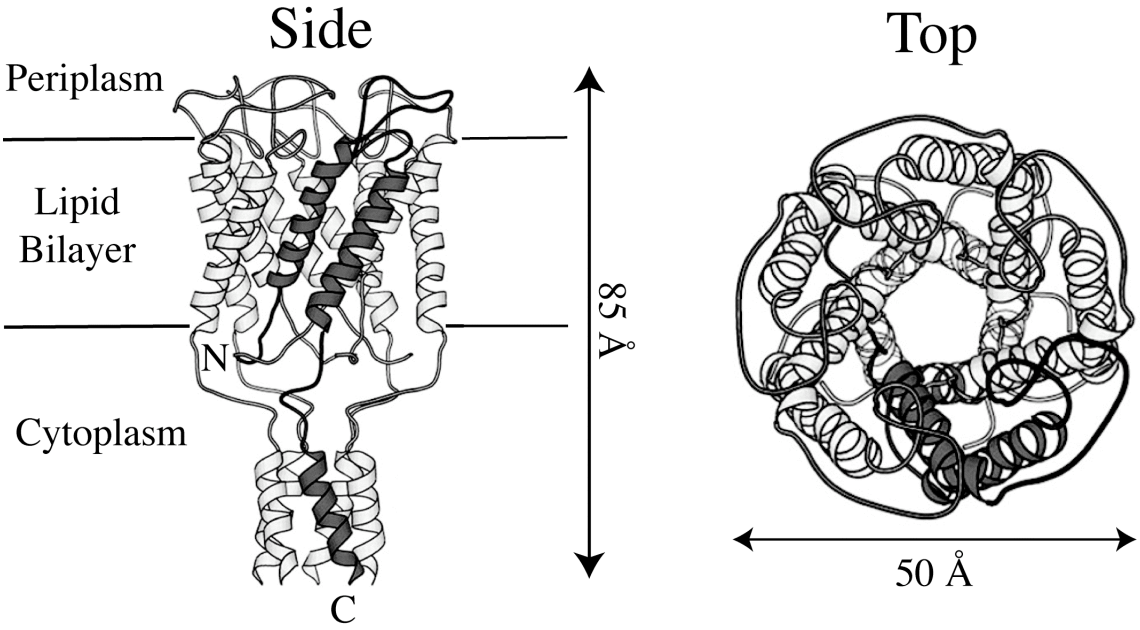

Figure 1.1: Crystal structure of Tb-MscL. Left, the structure shows a homopentameric arrangement perpendicular to the lipid bilayer with a single subunit highlighted. Each subunit contains two TM α helices and a cytoplasmic α helix. N is the N-terminus and C is the C-terminus of a single subunit. Right, a view from the periplasmic region. Figure adapted from (12).

Synthetic MscL samples initially are dissolved in trifluoroethanol (TFE) and therefore must be reconstituted into a lipid bilayer in order to form functional channels. Lipids used in this research include: 1,2-Dioleoyl-*sn*-Glycero-3-Phosphocholine (DOPC) (Figure 1.2 A) and azolectin, an extract from soybean containing 40% phosphocholine lipid derivatives. For vesicle formation, lipid is first dried in order to create a lipid film (Figure 1.2 B, 1). The addition of water causes this lipid layer to swell and form bilayers. With agitation multilamellar vesicles (MLVs) are formed (Figure 1.2 B, 2). MLVs can then be extruded through filters of specific diameters to form large unilamellar vesicles

(LUVs) or can be sonicated to form small unilamellar vesicles (SUVs) (Figure 1.2 B, 3 & 4) (13). Giant unilamellar vesicles (GUVs) are formed by the electroformation technique (14,15), which applies an oscillating electrical current with a geometric wave function (Figure 1.2 B, 5).

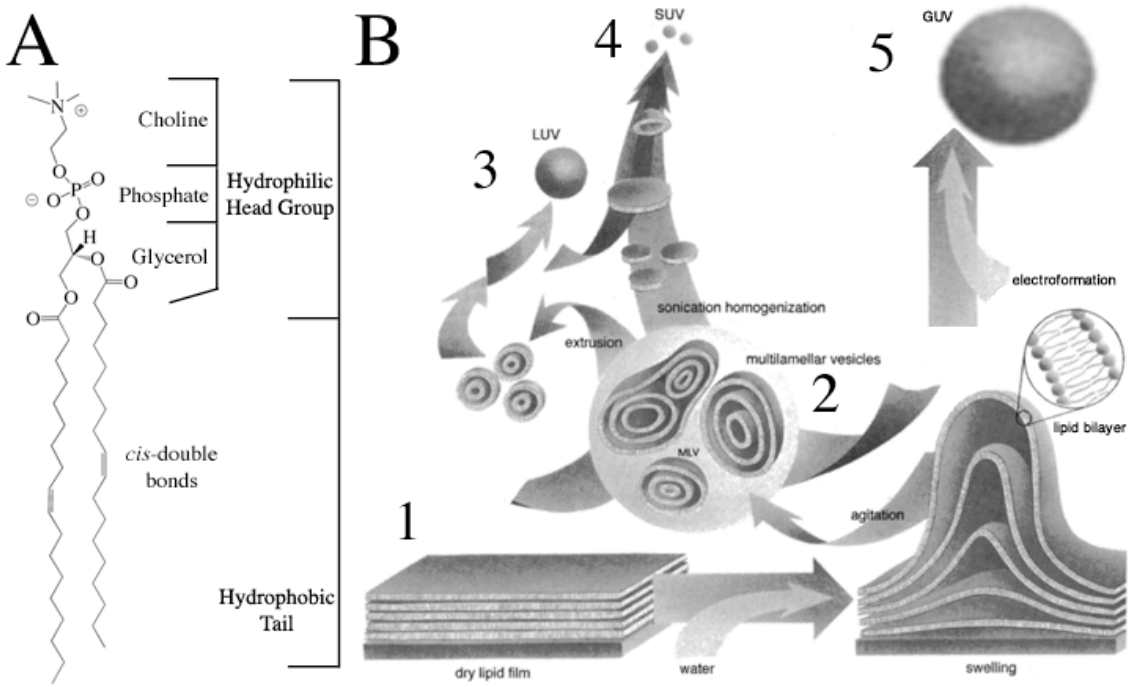

Figure 1.2: Diagram of a DOPC lipid and vesicle formation. (A) DOPC structure is shown with the hydrophilic head group and hydrophobic tail groups highlighted. (B) Vesicle formation. 1) The dried lipid film is shown and is the start of vesicle formation. 2) Upon addition of water the lipid swells and forms MLV upon agitation. 3) Extrusion of MLVs creates LUVs. 4) Sonication of MLVs creates a homogenous population of SUVs. 5) Electroformation of the dry lipid film when placed in water forms GUVs. Figure on right adapted from (13).

Many methods exist for incorporation of membrane proteins into vesicles, including organic solvent-mediated reconstitution, mechanical reconstitution, detergent-mediated reconstitution, and dried lipid-protein reconstitution. Organic solvent-mediated reconstitution has been used to incorporate rhodopsin into LUVs (16), but the organic solvents quickly degrade many membrane proteins (17). Mechanical reconstitution uses

force to fragment a bacterial cell and then fusion is allowed to occur with prepared MLVs. This method has been used for MscL preparations (18), but is not useable for a completely synthetic protein. Detergent-mediated reconstitution is the most successful and widely used procedure for reconstitution of membrane proteins into vesicles. Membrane proteins are purified, solubilized in an aqueous-detergent solution, and applied to a dry lipid film. MLVs containing lipid, protein, and detergent are then subjected to dialysis or polystyrene beads to selectively remove detergent (17,19). Detergent can alter the physical state of vesicles (20) and results in loss of reproducible gigaohm (GΩ) seals necessary for electrophysiological characterization (18). Dried lipid-protein reconstitution involves the drying of both the lipid and protein and then forming vesicles. This method has been successfully used for the incorporation of gramicidin channels (21) and MscL (11).

1.2 Results

1.2.1 Vesicle Reconstitution of Synthetic MscL

Four different methods have been used for vesicle reconstitution of synthetic MscL, three of which will be discussed here. The fourth method was published recently and used a modified dried lipid-protein reconstitution technique (21) of drying MscL onto lipid and then forming unilamellar blisters by the addition of Mg^{2+} (11). The MLV preparation was developed by Dr. Joshua Maurer and found to have the pentameric oligomer state when cross-linked (Figure 1.3, A). Briefly, solubilized B-Tb-MscL in the detergent *n*-dodecyl β-D-maltoside (DDM) was used, and MLVs were formed by rehydration of dry DOPC (20). SUVs were formed upon selective removal of DDM

using polystyrene Bio-Beads and MLVs were then formed by the freeze-thaw technique (20,22). Removal of DDM is necessary to avoid thread-like micelles, open bilayer structures (19), and to obtain GΩ seals for patch clamp recording (18).

The electroformation technique initially developed by Angelova and Dimitrov was used to create GUVs (14,15). A Pt wire electrode chamber was hand made to create GUVs. The MLV preparation was dried on the Pt wires and a sine wave of 2 V at a frequency of 10 Hz was applied for one hour as previously described (23). A second indium tin oxide (ITO) coverslip chamber was also hand made, to create more uniform GUVs, in collaboration with Sean Gordon. Synthetic MscL was dried onto a previously dried lipid film (11) and a square wave voltage of 1.5 V at 10 Hz was applied for 1 h (24).

The MLV preparation was the easiest initial route for synthetic MscL characterization because the procedure was previously determined, and the observation of pentameric channels suggested functionally reconstituted MscL (Figure 1.3 A). The addition of concentrated Mg^{2+} to the MLVs was hoped to form blisters that could be used for electrophysiological recording (11,18). While SUVs and LUVs are unilamellar, they can't be used for electrophysiology because they are not large enough compared to the electrode opening and are not visible under a microscope (18). The electroformation technique was used to create GUVs that would be readily visualized under a microscope and amenable to patch-clamp analysis.

1.2.2 Electron Microscopy of B-Ec-MscL in MLVs

Electron microscopy (EM) on MLVs prepared with B-Ec-MscL was performed to visualize the membrane protein in the lipid bilayer through the binding of streptavidin-

coated gold beads to the N-terminal biotin moiety. MLVs were prepared containing B-Ec-MscL and without, as a control for non-specific labeling. Electron micrographs of MLVs showed many vesicles were ruptured and damaged when compared to light microscopy images (data not shown). Gold particles showed a random labeling pattern with no statistical difference between the control MLVs (data not shown). After two labeling trials, EM was abandoned because of a lack of uniform labeling required to demonstrate that B-Ec-MscL was reconstituted into the MLVs.

1.2.3 Oligomeric State of MscL Analyzed by Cross-Linking in MLVs

The crystal structure of Tb-MscL shows a homopentameric arrangement (6). Tb-MscL lacks any native cysteine residues for cross-linking and mutations would be necessary, which could alter channel organization. Lysines 99 and 100 form a cluster of charged residues in the cytoplasmic region of the structure and are ~ 7 Å from the neighboring subunit counterparts. This proximity allows for the cross-linking of the primary amines using disuccinimidyl suberate (DSS), with a spacer arm of 11.4 Å, as previously described (6).

The MLV and cross-linking method developed by Dr. Joshua Maurer showed a pentamer when DSS was added to B-Tb-MscL (Figure 1.3, A Lanes 2–4) similar to the cross-linking experiments performed by Rees and co-workers (6). Surprisingly, B-Tb-MscL shows some dimeric protein without DSS (Figure 1.3, A Lane 1). Achieving only a pentameric cross-linking was highly dependent on the amount of time the labeling was allowed to proceed (Dr. Joshua Maurer, personal communication). Figure 1.3, B Lanes 2–5 show cross-linking experiments using the same procedure with both B-Ec-MscL and Tb-MscL and show oligomer states higher than a pentamer. While B-Ec-MscL shows

nearly the same cross-linking with 1.5 and 3 μg B-Ec-MscL (Figure 1.3, B Lanes 2 & 3), the B-Tb-MscL samples show varying cross-linking with 1.5 and 3 μg of B-Tb-MscL (Figure 1.3, B Lanes 4 & 5). The variation in cross-linking shows the dependence on the amount of protein in the sample and shows the limitation in determining the number of subunits in an ion channels. Hexameric states have been previously reported in the literature based on cross-linking and EM (25,26). As a control, cross-linking was performed on proteins that were solubilized in DDM micelles, and no cross-linking was observed (Figure 1.3, B Lanes 6–9).

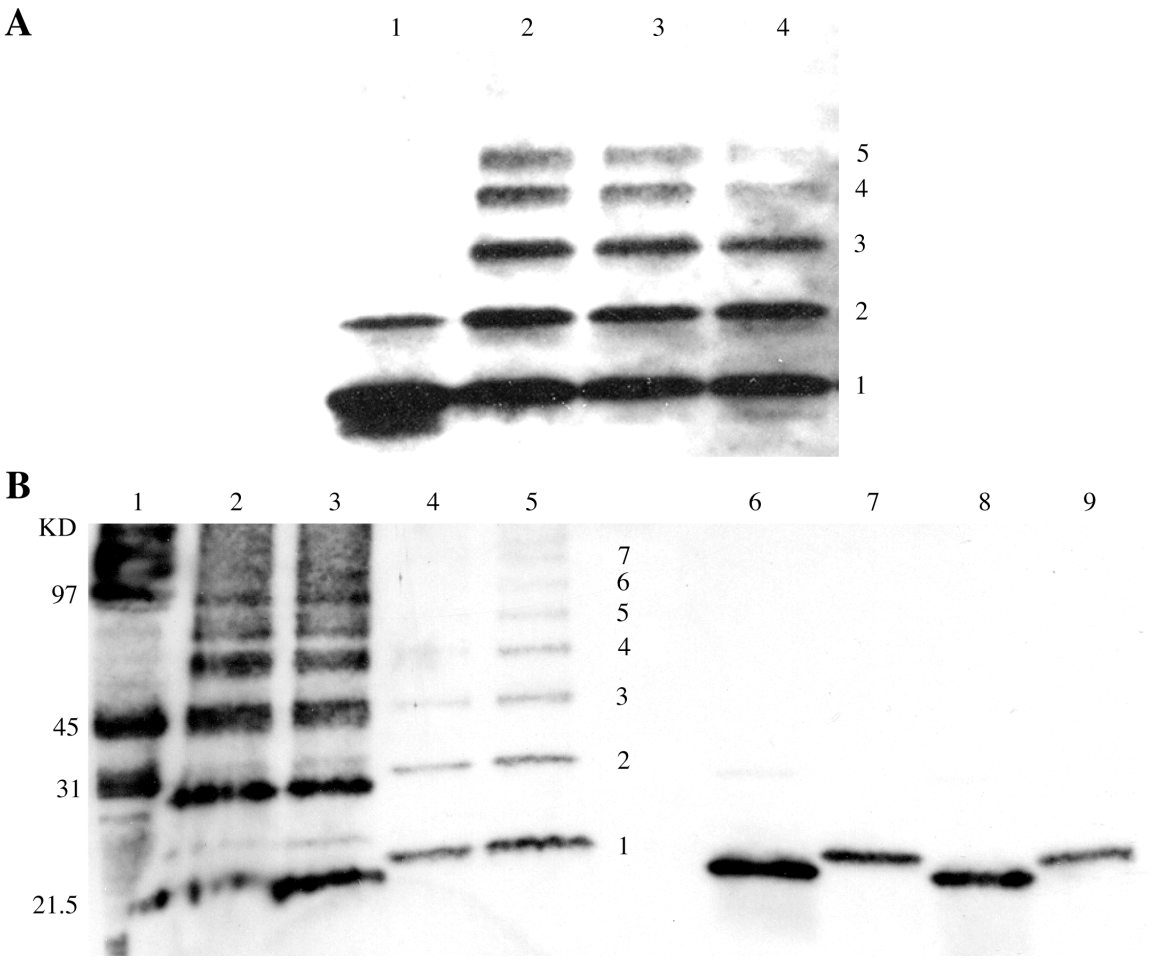

Figure 1.3: Oligomeric analysis of MscL using DSS cross-linking in MLVs. (A) Pentameric arrangement of B-Tb-MscL when incorporated into MLVs. Lane 1, B-Tb-MscL (2 μg) without DSS. Lanes 2–4 are B-Tb-MscL (3 μg) with DSS. Numbers to right represent number of subunits cross-linked. (B) Increased oligomers found when trying to replicate A. Lane 1, biotinylated molecular weight markers. Lane 2, B-Ec-MscL (1.5 μg) with DSS. Lane 3, B-Ec-MscL (3 μg) with DSS. Lane 4, B-Tb-MscL (1.5 μg) with DSS. Lane 5, B-Tb-MscL (3 μg) with DSS. Lanes 6 & 8, B-Ec-MscL (1 μg) solubilized in DDM without and with DSS, respectively. Lanes 7 & 9, B-Tb-MscL (1 μg) solubilized in DDM without and with DSS, respectively. Numbers in the center represent number of subunits cross-linked.

Reese and co-workers previously used the same technique for both Ec-MscL (3 μg) and Tb-MscL (10 μg), and the pentameric state was detected by staining with Coomassie brilliant blue (6). Coomassie brilliant blue has a detection limit of 0.1–0.5 μg of protein (Amersham), while NeutrAvidin, HRP conjugated is at least 5 orders of

magnitude more sensitive with a detection limit of 0.05–1 pg of protein (Pierce). Therefore altering the detection may yield a similar pentameric oligomer state, but would give no definitive means for knowing the functional state of synthetic MscL within the MLVs.

1.2.4 Fluorescence Imaging

MLV preparations containing B-Ec-MscL, TFE (no protein), and biotinylated lipid (B-DHPE) were used for fluorescence labeling with streptavidin conjugated to AlexaFluor488 (streptavidin-AlexaFluor488). Initial fluorescence on MLV preparations with these three preparations failed to yield any differences between the three samples (data not shown). Labeling was performed using a sevenfold excess and caused a large degree of background labeling on the MLVs. The labeling procedure also involved removal of excess fluorophore by three freeze-thaw cycles, centrifugation, and resuspension, which causes the MLVs to aggregate and encapsulate non-specifically bound streptavidin-AlexaFluor488 (27).

B-Ec-MscL was then labeled with more biotin moieties using EZ-Link Sulfo-NHS-LC-Biotin (NHS-B), which reacts with the primary amine on lysine residues. The spacer arm is 22.4 Å, further than the N-terminal biotin, and would allow for multiple biotins on a single subunit. MLV preparations with B-Ec-MscL, TFE, and B-DHPE were treated with NHS-B and labeled with streptavidin-AlexaFluor488.

Figure 1.4 displays the results of this labeling trial and conditions are labeled above each column. Figure 1.4, row A shows vesicles formed with TFE and no protein. The fluorescence detected after exposure times of 200 ms and 1,000 ms shows no intensity change, and fluorescence is due to small amounts of fluorophore present in

solution and/or non-specifically bound to the vesicles. Figure 1.4, row B shows vesicles containing B-DHPE (same moles as B-Ec-MscL shown in Figure 1.4, C & D). The image at 200 ms exposure time shows high concentration of streptavidin-AlexaFluor488 bound to the vesicles (see Figure 1.4, B overlay) and exposure of 1,000 ms completely saturates the image. B-Ec-MscL MLVs are shown in Figure 1.4, and rows C & D exhibit very high fluorescing points along the surface of the vesicles. The lipid bilayer is not as uniformly labeled as in Clayton *et al*. (11), but illustrates a differential labeling among the controls and the vesicles containing B-Ec-MscL. Biotinylated lipid exhibits the highest fluorescent intensity and illustrates that the streptavidin-AlexaFluor488 is specifically labeling accessible biotin (Figure 1.4, row B), but B-Ec-MscL shows less fluorescence, suggesting the N-terminal biotin and lysine coupled biotin are less accessible to the streptavidin-AlexaFluor488 and/or the proteins are localizing to specific areas on the vesicles.

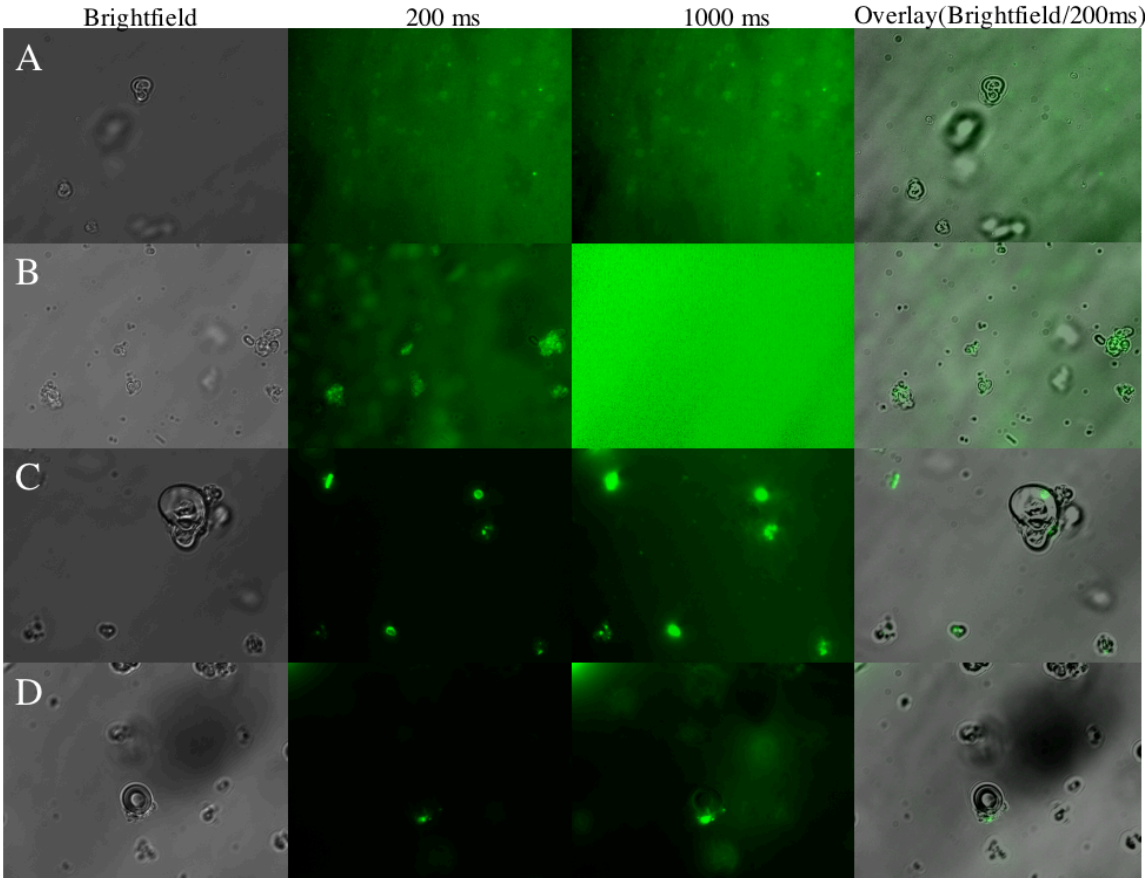

Figure 1.4: Fluorescence imagining of B-Ec-MscL in MLVs. All MLVs were subjected to the same procedure for additional labeling of biotin using NHS-B. Row A, Control MLVs lacking B-Ec-MscL (TFE only). Row B, MLVs containing biotinylated lipid (equivalent moles to B-Ec-MscL shown in C & D). Rows C & D, B-Ec-MscL containing MLVs. The far left column is imaging in brightfield. The two middle columns show fluorescence measurements with the exposure times listed above each column. The far right column is an overly of the brightfield and fluorescence image (200 ms).

GUV fluorescence images were prepared using a lower concentration of streptavidin-AlexaFluor488 that was allowed to diffuse throughout the sample as described (11). Figure 1.5, A, D, and G–I show brightfield images of GUVs created using a 100 Hz frequency rather than 10 Hz. This frequency was chosen because the vesicles form in larger aggregates of GUVs, which are easier to locate. Note the unilamellar vesicles appear to have very thick bilayers due to the diffraction of light. Figure 1.5, B and C show a GUV fluorescing along the lipid bilayer and also show an

altered structure when compared to other brightfield GUVs. Many images showed large aggregates of streptavidin-AlexaFluor488 present along the vesicle surface (shown in Figure 1.5, E and F). However most GUVs showed no fluorescence (Figure 1.5, G–I) and were similar to the TFE control (data not shown).

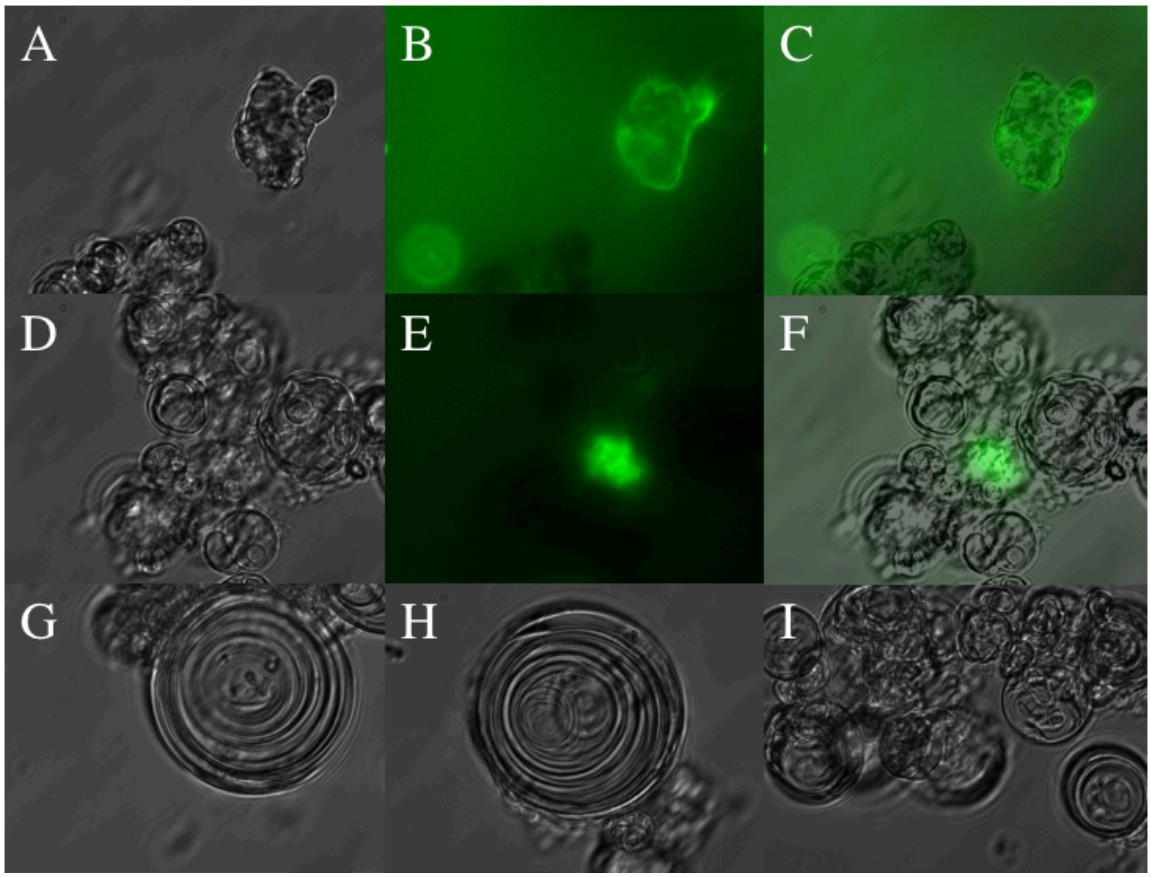

Figure 1.5: Fluorescence imaging of B-Ec-MscL GUVs prepared with Pt wire electrodes. (A & D) Brightfield images of B-Ec-MscL incorporated into GUVs. (B & E) Fluorescence images exposed for 100 ms. (C & F) Overlay of brightfield and fluorescence images. (G–I) Brightfield images of B-Ec-MscL incorporated in GUVs that showed no fluorescence.

The ITO coverslip GUV preparation was done in collaboration with Sean Gordon, who took all fluorescent images (Figure 1.6). DOPC GUVs were prepared by ITO coverslip electroformation and are shown in Figure 1.6, row A. The GUVs are labeled

with a hydrophobic fluorophore, DiI, which only fluoresces when incorporated into the lipid bilayer. Figure 1.6, B shows labeling of B-Ec-MscL incorporated into azolectin GUVs by perfusion of streptavidin-AlexaFluor488. The streptavidin-AlexaFluor488 is maintained outside of the vesicles throughout the labeling process, which is similar to vesicles perfused with AlexaFluor488 dye alone (data not shown). Figure 1.6, C shows B-Ec-MscL incorporated in azolectin GUVs washed with 1 mL of 1 X PBS. Fluorescent labeling is seen across all the lipid membranes, suggesting that the protein is distributed uniformly in the GUVs.

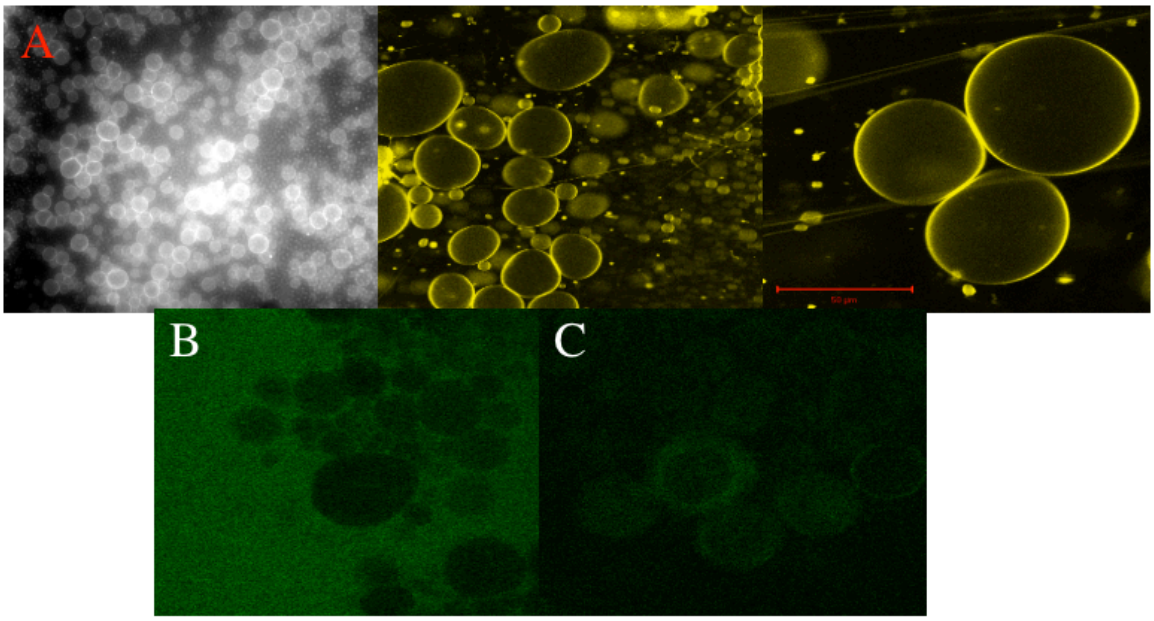

Figure 1.6: GUVs prepared by ITO coverslips and fluorescence imaging. (Row A) From left to right, DOPC GUVs under brightfield, fluorescence from DiI excitation, and fluorescence from DiI excitation zoomed in. Scale bar is 50 μm. Lower row is B-Ec-MscL incorporated in azolectin GUVs. (B) Perfusion with streptavidin-AlexaFluor488. (C) B-Ec-MscL incorporated in azolectin GUVs after wash with 1 X PBS to remove excess streptavidin-AlexaFluor488.

1.2.5 Electrophysiological Characterization of Pt Wire GUVs

Samples were prepared using DOPC and azolectin by the MLV preparation method, which reconstitutes B-Ec-MscL using DDM. After removal of the detergent using Bio-Beads, the samples were spread across the Pt wire and allowed to dry. Samples were given to Dr. George Shapovalov for single-channel patch-clamp recording. DOPC GUVs could not be studied because of failure to attain giga-ohm (GΩ) seals. Azolectin GUVs containing B-Ec-MscL were able to attain GΩ seals and had similar channel activity to that reported for synthetic MscL (11). This clearly shows that B-Ec-MscL is incorporated in a functional state within the MLVs and subsequently into GUVs during electroformation with Pt wire electrodes. Interestingly the DOPC GUVs could not be recorded on, which is most likely due to the lipid composition of the membrane.

1.3 Discussion

The functional reconstitution of synthetic MscL was achieved through the use of the DDM-mediated reconstitution in MLVs and subsequent electroformation to create GUVs, which was shown by single-channel patch-clamp study. GUVs prepared by ITO coverslips show greater uniformity in spherical shape than GUVs prepared by a Pt wire. The ITO GUVs also have a higher yield, remain fixed to the translucent coverslip, and recording can easily be analyzed by electrophysiology performed on the giant vesicles. Overall, the GUV methods offer a means for reconstitution of functional MscL protein for electrophysiological characterization and should be amenable for the incorporation of other ion channels and membrane proteins.

GUV preparations are an optimal method for characterization of proteins *in vitro* through single-channel recordings in the absence of other proteins present within cells. KcsA, a tetrameric K^+ channel, translated *in vitro* in the presence of LUVs was found to incorporate selectively within the lipid bilayer of LUVs (28). MscL and other simple homomeric prokaryotic ion channels may also spontaneously assemble into LUVs. Using this system along with nonsense suppression (29), unnatural amino acids could be selectively incorporated in MscL without the need for purification and GUVs could be made from LUVs. Many loss of function and gain of function MscL mutants were identified using a high throughput assay for channel function (30), but many of these mutations had drastic alterations in sterics or electrostatics when compared to the native amino acids. Unnatural amino acids could be incorporated at identified positions that are important for channel function and allowing analysis of specific interactions in more detail by electrophysiological characterization. Incorporation of fluorescent unnatural amino acids could also be utilized for fluorescence resonance energy transfer to gain dynamic information of ion channel function during gating.

1.4 Experimental Methods

1.4.1 Synthetic B-Ec-MscL Samples

B-Ec-MscL samples were chemically synthesized as described (11). Briefly, a modified native-chemical ligation technique was utilized to synthesize the full-length Ec-MscL with a biotin moiety placed at the N-terminus of the protein. Cysteine was substituted for glutamine 56 and asparagine 103 for the native-chemical ligation and selectively modified with bromoacetamide to produce side chains similar to native amino

acids in sterics and containing a terminal amide group. B-Tb-MscL was synthesized in a similar manner, substituting cysteine residues at glutamate 102 and serine 52 and masking with appropriate reagents. All samples were synthesized at Gryphon Therapeutics.

1.4.2 MLV Preparation and DDM-Mediated Reconstitution of B-Ec-MscL

10 X Rehydration Buffer (RB) (2.5 mM KCl, 1 mM EDTA, 50 mM HEPES, pH 7.2) was prepared and diluted as necessary. 79.8 μl DOPC in chloroform (Avanti Polar Lipids) was placed in a glass vial and rotoevaporated to dryness for 10 min. 5.4 mg of DDM (Anatrace) was added to 1 mL 1 X RB (.5% DDM solution). 20.7 μl of B-Ec-MscL in TFE (2 mg / mL) was placed into 220 μl of .5% DDM solution and was directly added to the vial containing dried DOPC. The B-Ec-MscL / .5% DDM / TFE solution was agitated at room temperature for 5 h to allow for MLV formation. 16 mg of degassed Bio-Beads SM Adsorbents (Bio-Rad) was added to the MscL / .5% DDM / TFE solution, to selectively remove DDM as described in (19,22), and agitated at room temperature for 7 h. This preparation gave a protein-to-lipid ratio of 1:300.

1.4.3 GUV Preparation With Pt Wire Electrodes

GUVs were prepared by the electroformation technique as previously described (14,15,23). The chamber (shown in Figure 1.7) was hand made by attaching two 5 cm X 2 mm Pt wires (Alfa Aesar) 2 mm apart from each other with epoxy glue on a glass slide. Epoxy glue was placed 1 mm around the length of the Pt wires to create a reservoir. 4 μl of the MLV preparation (described above) was spread across the Pt wires and dried under vacuum for 15 min. ~ 800 μl of 1 X RB was added to the chamber and a sine wave of 2 V at 10 Hz frequency was applied for 1 h through the Pt wires.

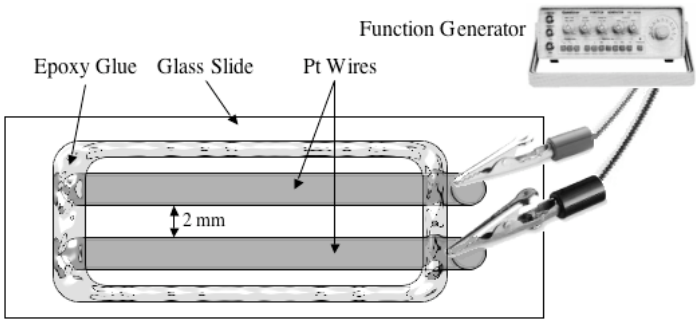

Figure 1.7: Diagram of Pt wire electrode chamber for GUV preparation.

1.4.4 GUV Preparation With ITO Coverslips

GUVs were prepared by the electroformation technique as previously described (14,15,24). GUVs are produced in varying diameter from 10 to 100 μm, with a mean diameter of 50 μm. The chamber (shown in Figure 1.8) was hand made by cutting a circle of 1.5 cm in a 35 X 10 mm plastic tissue culture dish (BD Biosciences). Coverslips were covered in a 75 Å layer of ITO (gift from Jerry Pine). 4 X .5 cm copper electrical conducting tape was attached to the ITO layer of two coverslips. The first coverslip was attached to the bottom of the tissue culture dish, centered under the circle to fully cover, with epoxy glue. Vacuum grease (Dow Corning) was spread around the circle to form a liquid barrier and to create a spacer for the second coverslip. 4 μl of 1 μg / ml DOPC in chloroform (Avanti Polar Lipids) or 1 μg / ml azolectin in chloroform (Sigma-Aldrich) was spread across the attached coverslip and air-dried for 20 min. For B-Ec-MscL reconstitution, 24 ng (1:5000 protein to lipid ratio) or 121 ng (1:1000 protein to lipid ratio) of B-Ec-MscL in TFE was smeared across the dried lipid on the coverslip and dried for 30 min under vacuum as previously described (11,21). ~ 300 μl millipore water was added to the chamber (to fill) and the second coverslip placed on top (making sure full

water contact is made throughout the area). A square wave voltage of 1.5 V at 10 Hz frequency was applied for 1 h through the copper electrical conducting tape.

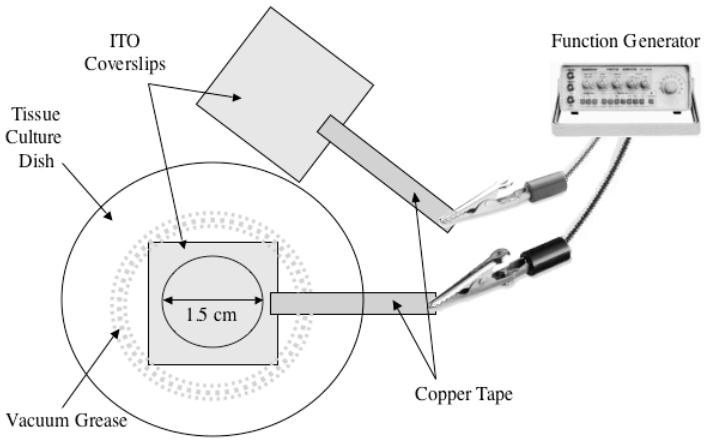

Figure 1.8: Diagram of ITO coverslip chamber for GUV preparation. (Top coverslip is placed on vacuum grease when square wave is applied.)

1.4.5 Electron Microscopy of B-Ec-MscL in MLVs

Samples were prepared as previously described (31). Copper grids were coated with collodion/carbon and evaporated under vacuum to be made hydrophobic (prepared by Pat Koen, Caltech Electron Microscope Facility). 10 μl of the MLV preparation (described above), with and without B-Ec-MscL, was labeled with 10 μl of AuroProbe EM Streptavidin G10 (Amersham Biosciences) with agitation for 12 h. The total sample (20 μl) was placed on the copper grid and allowed to dry for 1 min. #5 Whatman filter paper was used to dry remaining solution by touching the edge of the copper grid. 30 μl of a 1% phosphotungstic acid (Sigma-Aldrich) was added to the grid, left for 30 sec, and dried with filter paper. 30 μl of a 2% uranyl acetate (Sigma-Aldrich) solution was added to the grid, left for 30 sec, and dried with filter paper. Grids were examined in a

transmission electron microscope (Philips 420) in the Caltech Electron Microscope Facility.

1.4.6 Cross-Linking of MscL in MLVs

8.7 μl (1.5 μg B-Ec/Tb-MscL) or 17.4 μl (3 μg B-Ec/Tb-MscL) of the MLV vesicle preparation (described above) was mixed with 2.5 or 5 μl of 8 mM DSS (Pierce), respectively. Samples were sonicated for 5 min at room temperature and quenched with 10 μl of urea gel loading buffer (50 mM TrisCl, pH 6.8, 2% SDS, 10% glycerol, 10 M urea, and .1% bromophenol blue). Samples were boiled for 3 min and subjected to SDS-polyacrylamide gel electrophoresis and transferred to nitrocellulose. Biotinylated SDS-PAGE standards (Bio-Rad) were run as a molecular weight marker. Standard Western blot procedures were used and protein was visualized using 45 μl NeutrAvidin, HRP conjugated (Pierce).

1.4.7 Fluorescence Imaging

30 μl of MLV preparations (B-Ec-MscL, TFE, & *N*-(biotinoyl)-1,2-dihexadecanoyl-*sn*-glycero-3-phosphoethanolamine (B-DHPE) (Molecular Probes) were prepared to pH = 8 with KOH. 0.83 μl of 10 mM EZ-Link Sulfo-NHS-LC-Biotin (Pierce) was added and incubated at room temperature for 3 h. 6 μl of 0.1 mg / ml streptavidin-AlexaFluor488 (Molecular Probes) in 1 X PBS was added and agitated for 12 h. Samples were sequentially freeze-thawed 3 times, centrifuged 5 min, supernatant was removed, and MLVs were resuspended in 35 μl of 1 X RB. 2 μl of 0.1 mg / ml streptavidin-AlexaFluor488 (Molecular Probes) in 1 X PBS was added to 400 μl of Pt wire GUV preparation containing B-Ec-MscL (made at 100 Hz) and labeling was allowed to proceed for 1 h. Fluorescence was observed on an Olympus IX71 inverted

microscope equipped with a shuttered 175 W xenon arc lamp, 488 nm excitation filter, a 515 nm fluorescence cube, and an Olympus Plan Apo 60X /1.4 numerical aperture oil immersion objective. Images were recorded using a Photometrix CCD camera.

ITO coverslip prepared GUVs were made with 15.7 μg of DOPC and 0.19 μg DiI (Molecular Probes), from 5 mM stock solution in chloroform, and B-Ec-MscL as described above with 1:5000 or 1:1000 protein-to-lipid ratio. B-Ec-MscL GUVs were labeled by perfusion of 500 μl of 10 ng / μl streptavidin-AlexaFluor488. Fluorescence images were taken at this point (Figure 1.6, B) and then vesicles were washed with 1 mL of 1 X PBS. Fluorescence was observed on a Zeiss LSM Pascal Inverted confocal microscope equipped with an Ar Laser (488 nm, 25 mW), two-channel fluorescence/reflection, and motorized XY scanning stage. Images were acquired at 12 bit per channel and processed using Zeiss LSM v.3.0sp2. (Caltech Biological Imaging Center).

1.4.8 Electrophysiological Characterization of Pt Wire GUVs

GUVs were prepared with the Pt wire chamber (described above). B-Ec-MscL GUVs were prepared with either DOPC or azolectin lipids. Single-channel recordings were made by Dr. George Shapovalov as described in Clayton *et al*. (11).

1.5 References

1. Perozo, E., and Rees, D.C. (2003) Structure and mechanism in prokaryotic mechanosensitive channels. *Curr. Opin. Struct. Biol.*, **13**, 432–442.

2. Sukharev, S.I., Blount, P., Martinac, B., and Kung, C. (1997) Mechanosensitive channels of *Escherichia coli*: the MscL gene, protein, and activities. *Annu. Rev. Physiol.*, **59**, 633–657.

3. Wood, J.M. (1999) Osmosensing by bacteria: Signals and membrane-based sensors. *Microbiol. Mol. Biol. Rev.*, **63**, 230–262.

4. Morbach, S., and Kramer, R. (2002) Body shaping under water stress: Osmosensing and osmoregulation of solute transport in bacteria. *Chembiochem.*, **3**, 384–397.

5. Sukharev, S.I., Blount, P., Martinac, B., Blattner, F.R., and Kung, C. (1994) A large-conductance mechanosensitive channel in *E. coli* encoded by mscL alone. *Nature*, **368**, 265–268.

6. Chang, G., Spencer, R.H., Lee, A.T., Barclay, M.T., and Rees, D.C. (1998) Structure of the MscL homolog from *Mycobacterium tuberculosis*: A gated mechanosensitive ion channel. *Science*, **282**, 2220–2226.

7. Maurer, J.A., Elmore, D.E., Lester, H.A., and Dougherty, D.A. (2000) Comparing and contrasting *Escherichia coli* and *Mycobacterium tuberculosis* mechanosensitive channels (MscL). New gain of function mutations in the loop region. *J. Biol. Chem.*, **275**, 22238–22244.

8. Sukharev, S.I., Sigurdson, W.J., Kung, C., and Sachs, F. (1999) Energetic and spatial parameters for gating of the bacterial large conductance mechanosensitive channel, MscL. *J. Gen. Physiol.*, **113**, 525–540.

9. Anishkin, A., Gendel, V., Sharifi, N.A., Chiang, C.S., Shirinian, L., Guy, H.R., and Sukharev, S. (2003) On the conformation of the COOH-terminal domain of the large mechanosensitive channel MscL. *J. Gen. Physiol.*, **121**, 227–244.

10. Shapovalov, G., Bass, R., Rees, D.C., and Lester, H.A. (2003) Open-state disulfide crosslinking between *Mycobacterium tuberculosis* mechanosensitive channel subunits. *Biophys. J.*, **84**, 2357–2365.

11. Clayton, D., Shapovalov, G., Maurer, J.A., Dougherty, D.A., Lester, H.A., and Kochendoerfer, G.G. (2004) Total chemical synthesis and electrophysiological characterization of mechanosensitive channels from *Escherichia coli* and *Mycobacterium tuberculosis*. *Proc. Natl. Acad. Sci. USA*, **101**, 1764–4769.

12. Spencer, R.H., and Rees, D.C. (2002) The alpha-helix and the organization and gating of channels. *Annu. Rev. Biophys. Biomol. Struct.*, **31**, 207–233.

13. Lasic, D.D. (1997) *Liposomes in Gene Delivery*. CRC Press LLC, Boca Raton, FL.

14. Angelova, M., and Dimitrov, D. (1986) Liposome electroformation. *Faraday Discuss. Chem. Soc.*, **81**, 303–308.

15. Dimitrov, D., and Angelova, M. (1988) Lipid swelling and liposome electroformation mediated by electric fields. *Bioelectrochem. Bioenerg.*, **19**, 323–333.

16. Szoka, F., Jr., and Papahadjopoulos, D. (1978) Procedure for preparation of liposomes with large internal aqueous space and high capture by reverse-phase evaporation. *Proc. Natl. Acad. Sci. USA*, **75**, 4194–4198.

17. Rigaud, J.L., Pitard, B., and Levy, D. (1995) Reconstitution of membrane proteins into liposomes: Application to energy-transducing membrane proteins. *Biochim. Biophys. Acta.*, **1231**, 223–246.

18. Delcour, A.H., Martinac, B., Adler, J., and Kung, C. (1989) Modified reconstitution method used in patch-clamp studies of *Escherichia coli* ion channels. *Biophys. J.*, **56**, 631–636.

19. Knol, J., Sjollema, K., and Poolman, B. (1998) Detergent-mediated reconstitution of membrane proteins. *Biochemistry*, **37**, 16410–16415.

20. Lambert, O., Levy, D., Ranck, J.L., Leblanc, G., and Rigaud, J.L. (1998) A new "gel-like" phase in dodecyl maltoside-lipid mixtures: Implications in solubilization and reconstitution studies. *Biophys. J.*, **74**, 918–930.

21. Lougheed, T., Borisenko, V., Hand, C.E., and Woolley, G.A. (2001) Fluorescent gramicidin derivatives for single-molecule fluorescence and ion channel measurements. *Bioconjug. Chem.*, **12**, 594–602.

22. Chami, M., Steinfels, E., Orelle, C., Jault, J.M., Di Pietro, A., Rigaud, J.L., and Marco, S. (2002) Three-dimensional structure by cryo-electron microscopy of YvcC, an homodimeric ATP-binding cassette transporter from *Bacillus subtilis*. *J. Mol. Biol.*, **315**, 1075–1085.

23. Sanchez, S.A., Bagatolli, L.A., Gratton, E., and Hazlett, T.L. (2002) A two-photon view of an enzyme at work: *Crotalus atrox* venom PLA2 interaction with single-lipid and mixed-lipid giant unilamellar vesicles. *Biophys. J.*, **82**, 2232–2243.

24. Kahya, N., Pecheur, E.I., de Boeij, W.P., Wiersma, D.A., and Hoekstra, D. (2001) Reconstitution of membrane proteins into giant unilamellar vesicles via peptide-induced fusion. *Biophys. J.*, **81**, 1464–1474.

25. Blount, P., Sukharev, S.I., Moe, P.C., Schroeder, M.J., Guy, H.R., and Kung, C. (1996) Membrane topology and multimeric structure of a mechanosensitive channel protein of *Escherichia coli*. *Embo. J.*, **15**, 4798–4805.

26. Saint, N., Lacapere, J.J., Gu, L.Q., Ghazi, A., Martinac, B., and Rigaud, J.L. (1998) A hexameric transmembrane pore revealed by two-dimensional crystallization of the large mechanosensitive ion channel (MscL) of *Escherichia coli*. *J. Biol. Chem.*, **273**, 14667–14670.

27. Sou, K., Naito, Y., Endo, T., Takeoka, S., and Tsuchida, E. (2003) Effective encapsulation of proteins into size-controlled phospholipid vesicles using freeze-thawing and extrusion. *Biotechnol. Prog.*, **19**, 1547–1552.

28. van Dalen, A., van der Laan, M., Driessen, A.J., Killian, J.A., and de Kruijff, B. (2002) Components required for membrane assembly of newly synthesized K^+ channel KcsA. *FEBS Lett.*, **511**, 51–58.

29. Dougherty, D.A. (2000) Unnatural amino acids as probes of protein structure and function. *Curr. Opin. Chem. Biol.*, **4**, 645–652.

30. Maurer, J.A., and Dougherty, D.A. (2003) Generation and evaluation of a large mutational library from the *Escherichia coli* mechanosensitive channel of large conductance, MscL: Implications for channel gating and evolutionary design. *J. Biol. Chem.*, **278**, 21076–21082.

31. Barnakov, A.N. (1994) Sequential treatment by phosphotungstic acid and uranyl acetate enhances the adherence of lipid membranes and membrane proteins to hydrophobic EM grids. *J. Microsc.*, **175**, 171–174.